

Vibration attenuation properties of piezoelectric metamaterial plates

A. Hosseinkhani^a, E. Rohan^a

^aDepartment of Mechanics, Faculty of Applied Sciences, University of West Bohemia, Univerzitní 8, 301 00 Plzeň, Czech Republic

1. Introduction

Metamaterials, due to their exceptional properties beyond those of conventional materials, find applications in various fields, including vibration control. One subset of metamaterials is Phononic Crystals (PCs), which are able to manipulate the propagation of elastic waves. PCs are constructed by periodically repeating a heterogeneous structure known as a unit-cell [3]. The feature that provides the ability of wave manipulation for a PC is called bandgap. Over the bandgap frequencies, the propagation of elastic waves can be stopped completely. Bandgaps are influenced by several parameters, such as geometrical and material properties. In this regard, different geometry and material optimization techniques have been employed in the literature on metamaterials to achieve the best performance in terms of bandgap frequencies [4, 5]. Once the PCs are integrated with piezoelectric materials, more options will be available to control the bandgap properties. An electric circuit (named shunting circuit) can be attached to such materials, and the bandgap features can be changed by the use of electrical properties [2].

In this study, a heterogeneous piezoelectric 2-D plate is considered. The heterogeneity provides the periodic structure with the antiresonance property inducing a non-dissipative damping within specific frequency ranges called bandgaps, where the standing or propagating waves are suppressed. This paper examines different mechanisms for controlling bandgap properties and investigates their influences on bandgap characteristics. Finally, the bandgaps are utilized for controlling the propagation of vibrational waves along the piezoelectric plate in the frequency domain.

2. Bandgap diagram and vibration attenuation

A phononic crystal consisting of a piezoelectric matrix and solid inclusions is considered, as shown in Fig.1. The bandgap diagram and the corresponding geometrical parameters are also presented in Fig.1. The chosen material for the matrix is PZT-5A, and for the inclusion a solid-soft material with mechanical properties of $E = 4 \cdot 10^8$ Pa, $\rho = 6500$ kg/m³, $\nu = 0.3$ is considered. In this context, 'soft inclusion' refers to a material whose elastic modulus is significantly lower than that of the matrix.

The governing equations of the solid and piezoelectric mediums are as Eqs. (1) and (2), respectively:

$$\rho \ddot{u}(r, t) - \nabla \cdot \sigma(u) = 0, \quad (1)$$

$$\begin{aligned} \rho \ddot{u}(r, t) - \nabla \cdot \sigma(u, \phi) &= 0, \\ -\nabla \cdot D(u, \phi) &= 0. \end{aligned} \quad (2)$$

The bandgap diagram is obtained from the dispersion analysis of these equations with the following Floquet-Bloch periodic boundary condition

$$u_{\square}(r + L) = u_{\square}(r)e^{ikL}, \quad (3)$$

where L is the periodicity length of the structure. Detailed descriptions about the evaluation of the bandgap diagram can be found in [1].

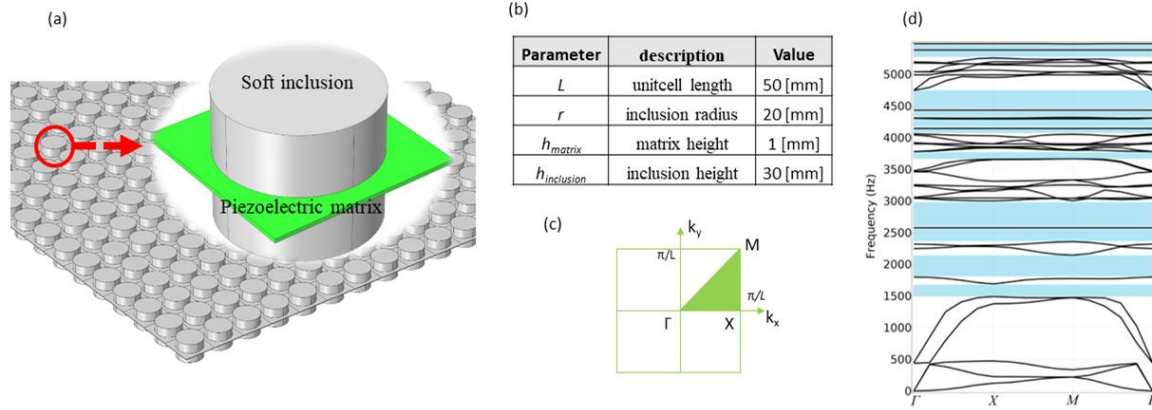


Fig. 1. (a) Schematic of the periodic structure and the unit-cell, (b) geometrical parameters (c) wave vectors and IBZ (d) the bandgap diagram

One critical geometrical parameter in this structure is inclusion height. As one example, the effects of this parameter, besides the schematic of the unit cell, are presented in Fig. 2 for three different heights: 1 mm, 15 mm, and 30 mm. As it is observed, no bandgap exists for the case of 1 mm, while some narrow bandgaps have appeared as the height is increased to 15 mm. By following the increase of height, more bandgaps with wider ranges are achieved. This validates the effects of inertia that increase with increasing height. Bandgaps are also shifted to lower frequencies as the height increases.

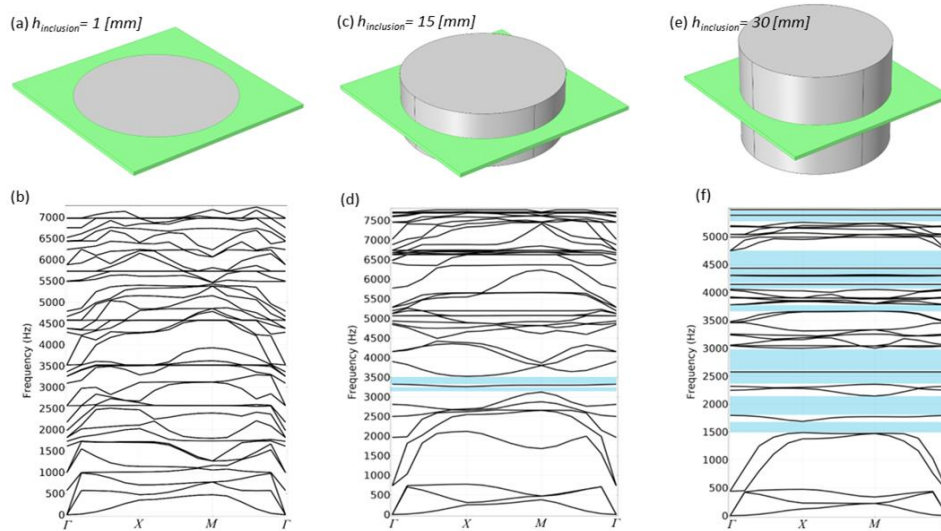


Fig. 2. Effects of inclusion height on the bandgap properties (a) $h_{inclusion} = 1$ mm, (b) $h_{inclusion} = 15$ mm, (c) $h_{inclusion} = 30$ mm

Then, a shunting circuit is connected to the piezoelectric element. Just a single resistor with the impedance of R (Ω) is considered to act as the shunting circuit (Fig. 3). As an example of the effect of the circuit on mechanical parameters, the elasticity matrix (c^{SU}) is calculated as the

inverse of the compliance matrix ($e^{SU}=(s^{SU})^{-1}$), and then its first component (E_{11}) is plotted versus electric resistance and frequency (Fig. 3b). As we can see, by changing the electric resistance, E_{11} changes about 50% (from $1.2 \cdot 10^{11}$ to $1.8 \cdot 10^{11}$). The shunting circuit changes the material properties and, accordingly, the bandgap properties.

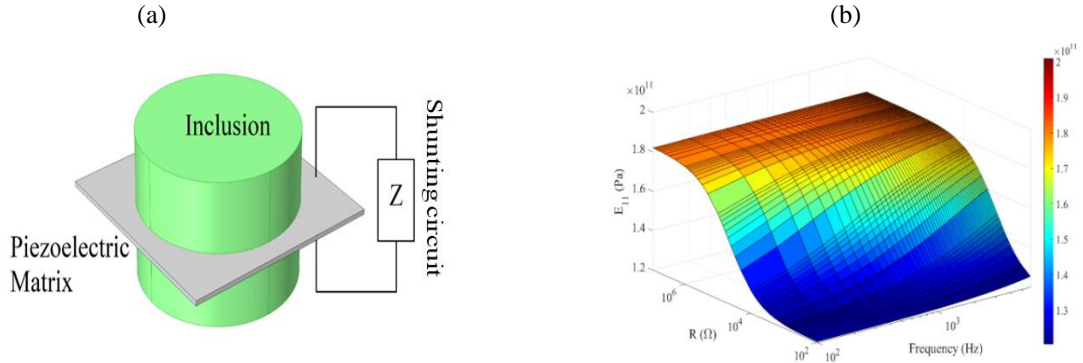


Fig. 2. (a) Schematic of the shunting circuit. (b) The variations of elasticity tensor component (E_{11}) with respect to electric resistance and frequency. (c) Variations of FBGOF and WFBG with respect to electrical resistance

Finally, the presented unit-cell is utilized in a finite structure and the vibration attenuation along the structure is investigated. Vibration attenuation is evaluated by defining the term Transmission Loss (TL) as $TL=20 \log(Y_{out}/Y_{in})$. The schematic of the finite meta-structure with the Periodic Boundary Conditions (P.B.C) and input as well as output points are depicted. TL is calculated and plotted beside the bandgap frequency ranges in Fig. 4. We can see that over the bandgaps, a big gain is achieved in TL for the meta-structure that is equivalent to no wave propagation.

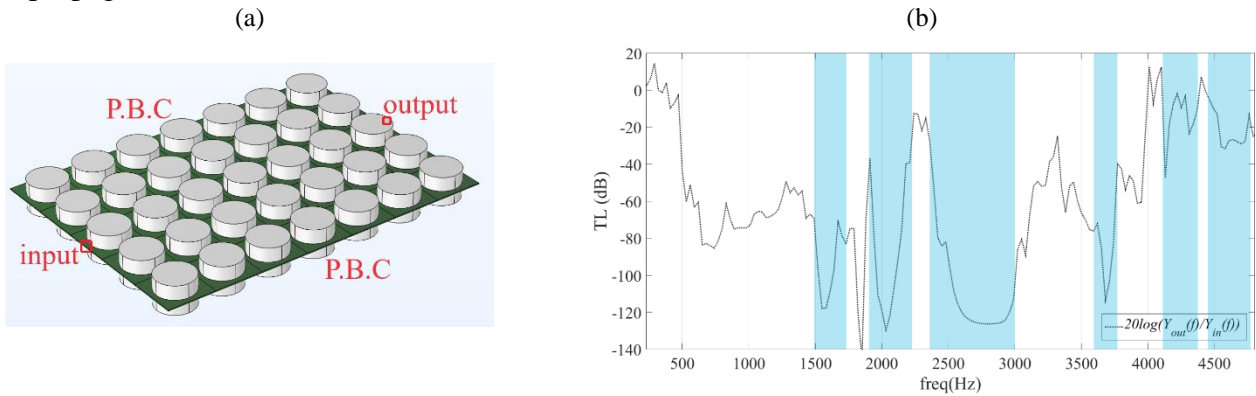


Fig. 4. (a) Schematic of the finite phononic crystal. (b) Transmission Loss diagram over the considered frequency range

3. Conclusion

A two-dimensional phononic crystal (a piezoelectric matrix interacting with soft inclusions) was investigated in this paper. The mechanisms of geometrical properties for controlling bandgap features and electrical properties for controlling the mechanical response were studied. The obtained results confirm the ability of such structures to control the propagation of vibrational waves, whereby more than 100 dB reduction was achieved over the bandgap frequencies.

Acknowledgement

The research was supported by the project GACR 23-06220S.

References

- [1] Deymier, P.A., Acoustic metamaterials and phononic crystals, Springer Science & Business Media, 2013.
- [2] Hagood, N.W. and Flotow, A.V., Damping of structural vibrations with piezoelectric materials and passive electrical networks, *Journal of sound and vibration*, (146) (2) (1991) 243-268.
- [3] Lu, M.H., Feng, L. and Chen, Y.F. "Phononic crystals and acoustic metamaterials." *Materials today*, (12) (12) (2009) 34-42.
- [4] Panahi, E., Hosseinkhani, A., Frangi, A., Younesian, D., and Zega, V., A novel low-frequency multi-bandgaps metaplate: Genetic algorithm based optimization and experimental validation, *Mechanical Systems and Signal Processing*, (181) (2022) 109495.
- [5] Vondřejc, J., Rohan, E., and Heczko, J., Shape optimization of phononic band gap structures using the homogenization approach, *International Journal of Solids and Structures*, (113) (2017) 147-168.